Laboratory measurements of remote sensing reflectance of selected phytoplankton species from the Baltic Sea

Oceanologia (2018) 60, 86—96

Available online at www.sciencedirect.com

ScienceDirect

journal homepage: www.journals.elsevier.com/oceanologia/

ORIGINAL RESEARCH ARTICLE

Laboratory measurements of remote sensing reflectance of selected phytoplankton species from the Baltic Sea

Monika Soja-Woźniak [a,b,c,*], **Mirosław Darecki** [d], **Bożena Wojtasiewicz** [a,e], **Katarzyna Bradtke** [a]

[a] *Institute of Oceanography, University of Gdańsk, Poland*
[b] *Department of Space, Earth and Environment, Chalmers University of Technology, Gothenburg, Sweden*
[c] *CSIRO Oceans & Atmosphere, Hobart, TAS, Australia*
[d] *Institute of Oceanology Polish Academy of Sciences, Sopot, Poland*
[e] *CSIRO Oceans & Atmosphere, Crawley, WA, Australia*

Received 19 May 2017; accepted 8 August 2017
Available online 26 August 2017

KEYWORDS
Phytoplankton monoculture;
Laboratory measurements;
Remote sensing reflectance

Summary Results of unique laboratory measurements of remote sensing reflectance (R_{rs}) of several phytoplankton species typically occurring in high abundances in the Baltic Sea waters are presented. Reflectance spectra for diatoms: *Cyclotella meneghiniana* and *Skeletonema marinoi* and cyanobacteria: *Dolichospermum* sp., *Nodularia spumigena* and *Synechococcus* sp. were analysed in terms of assessment of their characteristic features and the differences between them. These species contain similar pigments, which results in general similarities of reflectance spectra, i.e. decrease of reflectance magnitude in the blue and red spectrum regions. However, hyper-spectral resolution of optical measurements let us find differences between optical signatures of diatoms and cyanobacteria groups and between species belonging to one group as well. These differences are reflected in location of local maxima and minima in the reflectance spectrum and changes in relative height of characteristic peaks with changes of phytoplankton concentration. Wide ranges of phytoplankton concentrations were analysed in order to show the persistence of R_{rs} characteristic features. The picoplankton species, *Synechococcus* sp. show the

* Corresponding author at: CSIRO Oceans & Atmosphere, Hobart, TAS 7000, Australia. Tel.: +61 362 32 5163.
E-mail addresses: monika@soja-wozniak.com (M. Soja-Woźniak), darecki@iopan.gda.pl (M. Darecki), bozena.wojtasiewicz@ug.edu.pl (B. Wojtasiewicz), katarzyna.bradtke@ug.edu.pl (K. Bradtke).
Peer review under the responsibility of Institute of Oceanology of the Polish Academy of Sciences.

Production and hosting by Elsevier

http://dx.doi.org/10.1016/j.oceano.2017.08.001

most distinct optical signature, which let to distinguish separate cluster in hierarchical cluster analysis (HCA). The results can be used to calibrate input data into radiative transfer model, e.g. phase function or to validate modelled R_{rs} spectra.

1. Introduction

Harmful algal blooms that can vary in terms of their harmfulness, causal organisms, biomass distribution, and many other factors affecting the marine environment occur frequently in many marine and freshwater reservoirs. In the Baltic Sea massive phytoplankton blooms affecting its entire ecosystem are observed almost every year during spring, summer and early autumn (Kahru, 1997; Klais et al., 2013; Kutser et al., 2006; Pliński et al., 2007). From this point of view monitoring of these blooms, especially with cost effective methods like optical indirect measurements carried out in situ or remotely, e.g. by satellites, is in the interest of many environmental agencies and institutions. There is a strong demand for remote sensing algorithms which enable distinguishing between different phytoplankton species (IOCCG, 2014; Sathyendranath et al., 2016). Some of published studies use look up tables (LUT) (Xi et al., 2015) or optical indexes (Kim et al., 2016) based on modelled R_{rs} characteristics for individual species, but output of these models has not been validated against measured R_{rs}. The results presented here can be a significant contributions to that goal.

The spectral characteristic of the water leaving radiance (L_w) can be linked to the optically significant components of seawater. Thus the spectra of remote sensing reflectance (R_{rs}), being the ratio between the upwelling radiance just above the water and the downwelling irradiance at the sea surface, can be a useful tool which relates optical measurements to desired optically active seawater constituents (e.g. Darecki et al., 2008; Kratzer et al., 2008; Soja-Woźniak et al., 2017; Woźniak et al., 2008). For last two decades both in situ and remote sensing radiometry has developed significantly. Improved in situ techniques enabled measurement of L_w with hyperspectral resolution while bio-optical studies gave increasingly better understanding of the interaction between water components and the light field (Evers-King et al., 2014). Nowadays, retrieval of the phytoplankton pigments concentration based on R_{rs} can be obtained with reasonable accuracy (Darecki and Stramski, 2004; Darecki at al., 2008; Simis et al., 2005; Soja-Woźniak et al., 2017; Woźniak et al., 2016), but identification of single phytoplankton species or even entire phytoplankton functional groups by means of R_{rs} still remains a challenge (Craig et al., 2006; Hunter et al., 2008; Lubac et al., 2008; Shang et al., 2014; Torrecilla et al., 2011; Xi et al., 2015).

Phytoplankton species are characterised by their unique light absorption and backscattering properties resulting from differences in cell sizes and shapes, inner structure and composition of the pigments (e.g. Aguirre-Gómez et al., 2001; Vaillancourt et al., 2004; Whitmire et al., 2010) that all influence the shape of the R_{rs} spectra. The main pigments occurring in cyanobacteria and diatoms together with their absorptive properties are given in Table 1. Analysis of remote sensing reflectance of the Baltic Sea phytoplankton was carried out in the previous studies in order to detect and characterise algal blooms and to differentiate phytoplankton taxonomic groups (e.g. Kutser et al., 2006; Xi et al., 2015). However, the R_{rs} has been determined using either the R_{rs} dependence on the absorption and backscattering given by Gordon et al. (1975) or radiative transfer simulations. This approach can lead to some errors resulting from the applied assumptions, e.g. the assumption of the shape of the scattering function which for the phytoplankton cultures can be much different from the average Petzold particle scattering function as shown by Volten et al. (1998). There have been several studies performed in which the R_{rs} spectra of various phytoplankton taxonomic were measured under controlled laboratory or semi-laboratory conditions (Table 2).

Table 1 Main pigments occurring in cyanobacteria and diatoms with the location of main absorption peaks (based on Roy et al., 1989). The "+" sign indicates the presence of the chosen pigment.

Pigment	Cyanobacteria	Diatoms	Location of main absorption peaks [nm]
Chlorophylls			
a	+	+	430–432, 662–666
c		+	442–457, 628–634
Carotenoids			
β-Carotene	+	+	451–454, 475–480
Myxoxanthophyll	+		472–478, 502–510
Zeoxanthin	+		449–454, 475–481
Diadinoxanthin		+	445–449, 475–479
Diatoxanthin		+	451–453, 478–480
Fucoxanthin		+	444–449, 467–475
Phycobilins			
Phycocyanin	+		620
Phycoerythrin	+		550
Allophycocyanin	+		650

Table 2 Overview of previous laboratory and semi-laboratory studies on the characteristics of remote sensing reflectance spectra of selected phytoplankton species.

Group	Species	Tank volume [m^3]	Light conditions	Chl-*a* [mg m^{-3}]	Reference
Chlorophyte	*Chlorella* sp.	80	Outdoor, clear sky	0.5–60	[a]
Chlorophyte	*Chlorella* sp. (with small amounts of other species)	9.5	Outdoor, clear sky	34–439	[a]
Cyanophyte	*Anabaena* sp.	0.57	500 W halogen lamp	12.7–58.3	[a]
Bacillariophyte	*Novicula minima*	30	1000 W halogen lamp	3–77	[a]
Dinophyte	*Prorocentrum minimum*	0.05	Outdoor, clear sky	785	[b]
Cyanophyte	*Synechococcus* sp.	0.05	Outdoor, clear sky	29.9	[b]
Cyanophyte	*Planktothrix agardhii*	0.002	500 W halogen lamp	0–105	[c]
Cyanophyte	*Microcystis aeruginosa*	0.002	500 W halogen lamp	0–95.6	[c]
Cyanophyte	*Anabaena flos-aquae*	0.002	500 W halogen lamp	0–136	[c]
Chlorophyte	*Scenedesmus* sp.	0.002	500 W halogen lamp	0–122	[c]
Bacillariophyte	*Cyclotella meneghiniana*	0.002	500 W halogen lamp	0–127	[c]

[a] Gitelson et al. (1999).
[b] Warner and Fan (2013).
[c] Oyama et al. (2010).

In this study we characterised the reflectance spectra for five phytoplankton species commonly present in the Baltic Sea, diatoms: *Cyclotella meneghiniana* and *Skeletonema marinoi* and cyanobacteria: *Dolichospermum* sp., *Nodularia spumigena* and *Synechococcus* sp. The aim of the study was to find the characteristic features of R_{rs} spectra which can be observed for selected species over a wide range of phytoplankton concentrations. The results can be used to calibrate input data into radiative transfer model, e.g. phase function (Woźniak, 2014) or to validate modelled R_{rs} spectra. Moreover, they can be used as reference data to compare with in situ measured R_{rs} spectra in order to find a dominant species in algal assemblages. Analysis of variability of R_{rs} spectra as a response to changes in the phytoplankton growth conditions (e.g. nutrient availability, light, temperature, etc.) affecting pigment composition as well as cell sizes was out of scope of this study, therefore further investigation is necessary.

2. Material and methods

2.1. Selected phytoplankton species

Five phytoplankton species were chosen for this study. *C. meneghiniana* is a cosmopolitan diatom species in the euphotic surface waters of the whole Baltic Sea. It exists seasonally in the Southern Baltic in algal communities in autumn and winter, and is a quantitatively important component of the blooming species (Lewandowska and Kosakowska, 2004; Pankow et al., 1990). *S. marinoi* is a centric diatom species with worldwide distribution, which blooms mainly in the temperate sea waters. It is highly abundant also in the Baltic Sea especially during the spring bloom. *S. marinoi* has an important role as a primary producer in the Baltic Sea and serves as a valuable source of energy for higher trophic levels. Therefore, studying this organism has a high ecological relevance (Godhe et al., 2006). *N. spumigena* and *Dolichospermum* sp. are filamentous, nitrogen-fixing cyanobacteria species that can float near the water surface and form dense algal blooms which can be seen from satellite level (Walsby et al., 1995). *N. spumigena* is one of dominant species in summer algal blooms in the Baltic Sea. Moreover, this species produces nodularin, a hepatotoxin which has a negative impact on other organisms (Mazur and Pliński, 2003; Mazur-Marzec et al., 2006). *Dolichospermum* sp. (before known as *Anabaena* sp.) is a co-occurring species during cyanobacteria blooms and can contribute significantly to the total biomass, especially in the northern part of the Baltic Sea. *Dolichospermum* sp. can produce microcystin and is potentially toxic (Kanoshina et al., 2003; Karlsson et al., 2005; Seppälä et al., 2007; Suikkanen et al., 2007). *Synechococcus* sp. is a non-motile and non-nitrogen fixing cosmopolitan picocyanobacteria species which is a significant contributor to phytoplankton biomass and primary productivity (Albertano et al., 1997).

Synechococcus sp. (AA-0091), *C. meneghiniana* (BA-0010) and *S. marinoi* (BA-0098) were taken from the Culture Collection of Baltic Algae. They were grown in batch cultures in F/2 medium in a culture chamber under controlled conditions at the temperature of 18°C and 16/8 h light/dark cycle. *N spumigena* (CCNP1403), and *Dolichospermum* sp. (CCNP1405) strains were taken from the Culture Collection of Northern Poland. The strains were cultured in BG11 medium with salinity of 7 PSU in a phytotron chamber under the irradiance of 14 μE m^{-2} s^{-1} in 12/12 h light/dark cycle with constant temperature of 22°C. All analysed phytoplankton species are characterised in Table 3.

2.2. Experimental setup and radiometric measurements

A series of radiometric measurements of water containing phytoplankton monocultures were undertaken in a large circular tank ($Ø$ = 1.2 m, h = 1.4 m, V = 1.6 m^3) under controlled darkroom conditions (Fig. 1). The size of the tank and its inner mat black colour minimised the influence of light

Table 3 Size, shape and main characteristic pigments (PC – phycocyanin, PE – phycoerythrin, Fuco – fucoxanthin) of studied phytoplankton species.

Species	Diameter [μm]	Height [μm]	Shape	Marker pigment
Nodularia spumigena	6–12	<100	Cylinder	PC
Dolichospermum sp.	4.5–11	<100	Chain of spheres	PC
Synechococcus sp.	2	–	Sphere	PC, PE
Cyclotella meneghiniana	10–35	8.4–22.4	Cylinder	Fuco
Skeletonema marinoi	2–10	4–21	Cylinder	Fuco

All size and shape data taken from Annex 1 in Olenina et al. (2006).

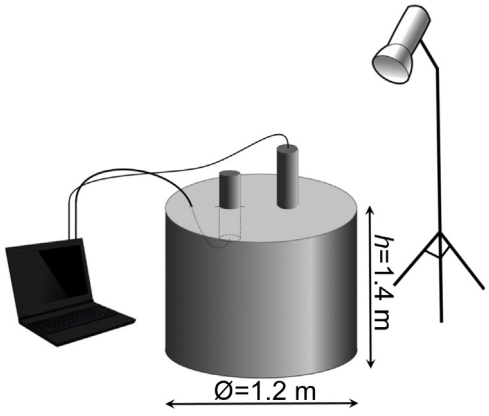

Figure 1 The experimental setup.

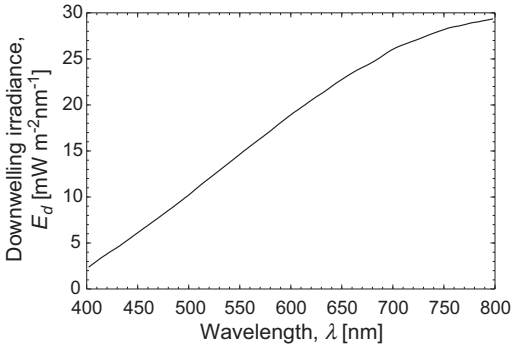

Figure 2 The irradiance spectrum of the lamp used during the measurements.

reflection from tank's sides and bottom on measurement results.

The experimental setup was illuminated only by an incandescent 2000 W lamp with smooth spectrum as an irradiance source (Fig. 2). It enabled to eliminate the influences of the variable contribution of the natural light in the background, moreover all measurements were taken under the same light conditions making the results comparable. The light intensity during the experiments was approximately 30 times lower compared to the daylight. Nevertheless, it was similar to the conditions in the culture chamber and therefore prevented formation of additional photo-protective pigments during the experiments.

During each series of measurements portions of phytoplankton monoculture were being added to brackish water (7 PSU equal to average salinity of the Baltic Sea surface waters; Feistel et al., 2010) in order to obtain increasing concentration of phytoplankton. Radiometric measurements were performed right after putting and carefully mixing the monocultures into the experimental tank. Downwelling irradiance (E_d) [W m^{-2} nm^{-1}] above (0^+) and below (at 0^-, 15 and 50 cm) the water surface and upwelling radiance (L_u) [W m^{-2} nm^{-1} sr^{-1}], just below water surface were measured with sampling intervals of 3.3 nm and a spectral resolution of ~ 10 nm by means of hand–held hyperspectral sensors RAMSES ACC–VIS (Trios) and RAMSES MRC (Trios), respectively (Hommersom et al., 2012). The radiometers have been mounted on the small frame to provide repeatability of sampling conditions. To minimise the self-shading effect, the MRC radiometer was custom designed with effective sensor diameter of 1 cm at the side of the optical window. The measurements were repeated five times for each concentration. The variability within these consecutive measurements varied among the species with the coefficient of variation (CV) (calculated separately for each wavelength as a ratio of standard deviation to mean value) ranging from 0.1 to 0.2% for E_d and 0.1 to 20% for L_u. The largest variability for L_u was observed between 450 nm and 470 nm and above 700 nm. In the range between 500 nm and 700 nm CV for L_u was lower than 10%. In further calculations mean values of E_d and L_u were used. In order to calculate the remote sensing reflectance, the upwelling radiance measured below the water surface $L_u(0^-)$ was transferred into the $L_u(0^+)$ by using immersion factor (I_f) determined for that radiometer in the paper (Zibordi and Darecki, 2006). Then remote sensing reflectance R_{rs} [sr^{-1}] in spectral range between 450 nm and 750 nm was derived as the ratio between L_u and E_d at the water surface (0^+). The diffuse attenuation coefficient of the downward irradiance $K_d(\lambda)$ [m^{-1}] was calculated as:

$$K_d(\lambda)(z_1, z_2) = -\frac{1}{z_2 - z_1} \ln\left(\frac{E_d(\lambda, z_2)}{E_d(\lambda, z_1)}\right), \quad (1)$$

where $E_d(z_i)$ is downwelling irradiance measured at z_i depth.

The transparency of water was characterised by K_d(PAR) calculated within the photosynthetically active radiation spectrum.

2.3. Pigment concentration

For each concentration of all analysed phytoplankton monoculture water samples were taken for further spectrophotometric analysis of chlorophyll-*a* (chl-*a*) (Jeffrey and Humphrey, 1975) and total carotenoids (TCar) concentrations (Parsons et al., 1984). Spectrophotometer Shimadzu UV-1202

UV–VIS was used. The pigment (chlorophyll-*a* and total carotenoids) concentration was calculated as follows:

$$C = (X \cdot E) \cdot V^{-1} (\mu g\, dm^{-3}), \quad (2)$$

where C is the chlorophyll *a* (chl-*a*) or total carotenoids (TCar) concentration, X is amount of pigment in μg per ml extract, E is the volume of acetone in ml (here 10 ml), and V is the volume of filtered water in litres. To calculate chlorophyll *a* (chl-*a*) concentration X was derived from the following equation:

$$X = (11.85 \cdot OD_{664} - 1.54 \cdot OD_{647} - 0.08 \cdot OD_{630}) \cdot L^{-1}, \quad (3)$$

where OD_λ stands for the optical density at particular wavelength corrected by subtracting OD_{750}. While to calculate total carotenoids (TCar) concentration X was derived from:

$$X = (7.6 \cdot (OD_{480} - 1.49 \cdot OD_{510})) \cdot L^{-1}, \quad (4)$$

where OD_{480} is the optical density at 480 nm corrected by subtracting $3 \cdot OD_{750}$, OD_{510} is the optical density at 510 nm corrected by subtracting $2 \cdot OD_{750}$. L is the pathlength of the cuvette in centimetres, here it was 1 cm.

2.4. Statistical approach

R_{rs} spectra measured for the highest phytoplankton biomass for each species were used as reference spectra to analyse how characteristic features change with decrease of phytoplankton concentration. The degree of similarity between the reference spectrum, and R_{rs} spectrum for each concentration of the same phytoplankton species was quantified with similarity index (SI) (e.g. Millie et al., 1997, 2002), which is given by:

$$SI = 1 - \frac{2\arccos(A)}{\pi}, \quad (5)$$

where A is a cosine of the angle between two vectors that comprise the fourth derivative of the two R_{rs} spectra (450–750 nm) smoothed with Savitsky–Golay filter. The SI calculation yields a number from zero to one, where zero indicates no similarity between reference and derived spectra, and one indicates absolute similarity between them. SI reflects mainly the differences in the spectral shape of optical data rather than magnitude.

The agglomerative hierarchical cluster analysis (HCA) was used in order to test which of the examined phytoplankton species gives an optical signal which is unique enough to differentiate this species from another one at different concentrations. This statistical method links entities (here, spectra derived from each species at different concentrations) characterised by similar properties into groups (clusters) (Jain et al., 1999; Townend, 2002). We tested R_{rs} and the 4th derivative of R_{rs} spectra as an input data in cluster analysis separately. The cluster tree was generated using Ward's method which ensures homogeneity (variance minimum) within a single group together with heterogeneity (variance maximum) among clusters (Nowacki and Jarosz, 1998). The similarity between groups is calculated from relative distance of linkage (Euclidean distance). The highest distance means 0% of similarity.

3. Results and discussion

E_d measured at three depths (0^- cm, 15 cm, 50 cm) were used to calculate K_d. For clear water three spectra of attenuation coefficient at different depth overlapped in the range between 415 nm and 740 nm. For shorter and longer wavelengths it showed minimal variation with a coefficient of variation (CV) not higher than 4% for all wavelengths. This allows us to assume that the results in studied range were not influenced by limited diameter of the tank. Together with increasing concentration of chlorophyll *a* the values of attenuation coefficient were increasing as well. However, the spectra of K_d for the layer between 0^- and 15 cm gave slightly lower values than for the layer between 0^- and 50 cm, or between 15 cm and 50 cm, what can be assigned to phytoplankton cells settling down during the radiometric measurements though carefully mixing. For all analysed phytoplankton species the highest coefficient of variation of K_d values measured in three layers was found for wavelengths around 550 nm and it was about 15%. Except *Cyclotella marinoi* which showed slightly higher values of CV, close to 20%, probably due to larger cell size comparing to other studied species. In further analysis K_d between 0^- and 50 cm was showed.

All analysed species contained chl-*a* and carotenoids but in different proportions (Table 4). The highest content of TCar was observed in *Synechococcus* sp. and *C. meneghiniana*, the lowest for *N. spumigena*. Attenuation coefficient at 490 nm (K_d(490)) showed good agreement ($R^2 = 0.82$) with chl-*a* concentration regardless phytoplankton species (Fig. 3). Therefore K_d(490) or $K_d(\lambda)$ at any other wavelength could not be a good candidate here for distinction between phytoplankton species. The transparency of water characterised by K_d(PAR) ranged from 1.1 to 7 m^{-1} (Table 4). Inverse of K_d(PAR) suggests that even for our lowest chl-*a* concentration the bottom effect can be omitted.

R_{rs} spectra measured for all species showed characteristic shape with decrease of reflectance in the blue and red regions. Different pigment composition for diatoms and cyanobacteria (Table 1) results in different location of local

Table 4 The range of measured parameters: concentration of chlorophyll *a* (chl-*a*) and carotenoids (TCar), ratio between concentration of carotenoids and chlorophyll *a* (chl-*a*:TCar), and attenuation coefficient within PAR (K_d(PAR)).

Species	Chl-*a* [mg m^{-3}]	TCar [mg m^{-3}]	Chl-*a*:TCar	K_d(PAR) [m^{-1}]
Nodularia spumigena	3–23	0.2–2	~10	1.6–2.7
Dolichospermum sp.	20–80	3–12	~7	1.7–5
Synechococcus sp.	25–60	10–26	~2.5	1.1–7
Cyclotella meneghiniana	9–23	4–10	~2.5	1.6–2.9
Skeletonema sp.	15–50	~4	~4.5–12	1.8–3.2

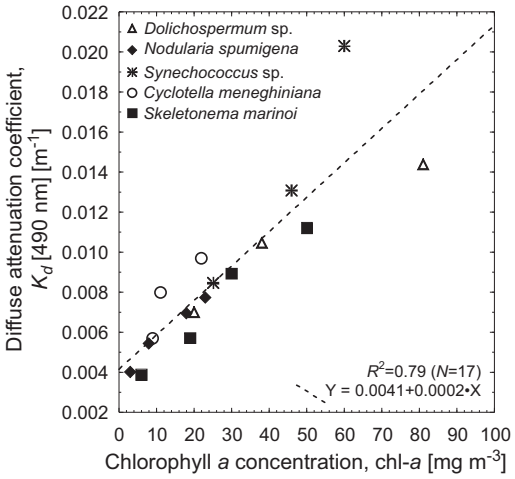

Figure 3 Relationship between chlorophyll *a* concentration and attenuation coefficient at 490 nm based on laboratory measurements.

maxima and minima in the reflectance spectrum (Fig. 4). Maximum of R_{rs} measured for cyanobacteria was located around 530–550 nm, whereas for diatoms could be seen around 570 nm what has been observed in previous studies (Metsamaa et al., 2006). $K_d(\lambda)$ spectra showed wider minimum for diatoms than for cyanobacteria (Fig. 4). Both groups contain pigments strongly absorbing in the range of 400–520 nm, as chl-*a* and carotenoids, which explains decrease of R_{rs} in this region. Additionally diatoms contain fucoxanthin with very wide absorption band from 450 to 540 nm (Wright and Jeffrey, 1987) and the maximum absorption between 450 and 470 nm. It resulted in a wider pigment absorption band for diatoms and R_{rs} maximum shifted towards longer wavelengths in comparison to cyanobacteria species. Among cyanobacteria, only R_{rs} spectrum of *Synechococcus* had a narrower peak around 530–550 nm. It also needs to be noted that it is a common feature that the position of phytoplankton pigment absorption minima and maxima in vivo are slightly shifted towards longer wavelengths relative to their position in solvents (Rabinowitch and Govindjee, 1969). This shift is not the same for different species. Therefore the location of R_{rs} minima and maxima for the analysed species was not the same, although most often being caused by the presence of the same pigments. Similarly to Gitelson et al. (1999) we observed a slight shift in the position of peaks with increasing phytoplankton concentration (Figs. 5 and 6).

In all analysed cyanobacteria a local minimum of R_{rs} at about 620 nm caused by absorption maximum of phycocyanin (PC) could be observed (Fig. 5). It was the most distinct for *Synechococcus* sp. Most probably *Synechococcus* sp. had very high PC to chl-*a* ratio among the analysed cyanobacteria species (Wojtasiewicz and Stoń-Egiert, 2016). This local minimum of R_{rs} was followed by local maximum, near 650 nm, very clearly seen by the peak in the 4th derivative spectrum (Fig. 5). It appeared mainly because it is located between two strong absorption bands (PC at 620 nm and chl-*a* at 670 nm). However, it could also be affected by PC fluorescence at 650 nm (e.g. Sobiechowska-Sasim et al., 2014). Such distinct peak was not observed in the diatom species we analysed. However, a small increase in this region could be seen, especially for the highest concentration of *S. marinoi* (Fig. 6). Most likely the occurrence of this peak was caused by the presence of chlorophyll $c_1 + c_2$ characterised by similar location of the second absorption peak to that of phycocyanin (Table 1). Similar differences in the spectral shape of R_{rs} were observed in the modelled results obtained by Metsamaa et al. (2006). In all analysed species a clear local minimum of R_{rs} accompanied by an increase in $K_d(\lambda)$ could be seen at 670 nm, which results from the presence of chl-*a* (Fig. 4). This minimum was followed by a maximum at about 700 nm which has been observed for both phytoplankton monocultures (e.g. Gitelson et al., 1999; Warner and Fan, 2013) and natural samples (e.g. Shang et al., 2014; Warner and Fan, 2013). This feature resulted from an interaction between light scattering by suspended particles and light absorption by water and chlorophyll *a* and its position was strongly correlated with chlorophyll *a* concentration moving towards longer wavelengths with increasing chl-*a* (e.g. Gitelson, 1992; Gitelson et al., 1999). Then the magnitude of R_{rs} decreased rapidly accompanied by an increase in $K_d(\lambda)$ which was caused by strong increase in pure water absorption in this part of the spectrum (Smith and Baker, 1981). In all our experiments we also observed a peak around 810 nm (data not shown). This feature was previously used to retrieve water constituents from remotely sensed data in turbid waters (Kutser et al., 2016), but in this study we mainly focused on the visible spectral range.

In the blue–green part of spectra the magnitude of R_{rs} decreased with increasing concentration of pigments (chl-*a* and TCar) in the case of the diatom *S. marinoi* (Fig. 6) and

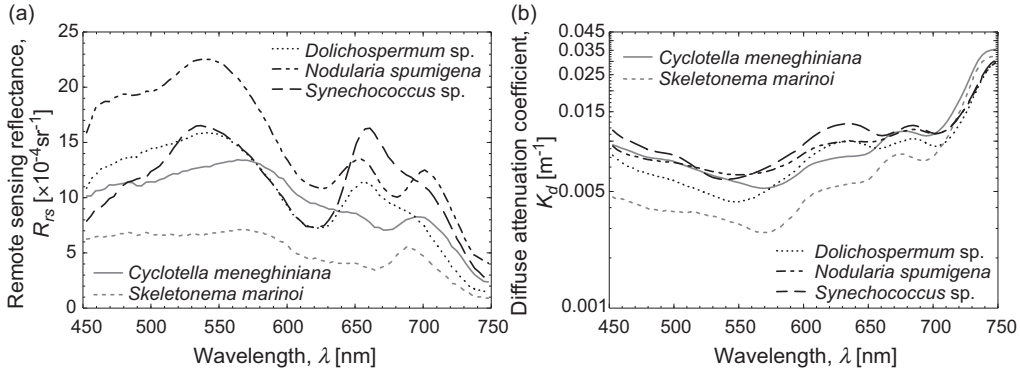

Figure 4 R_{rs} (*a*) and $K_d(\lambda)$ (*b*) spectra for studied phytoplankton species, chl-*a* for each was ~20 mg m^{-3}.

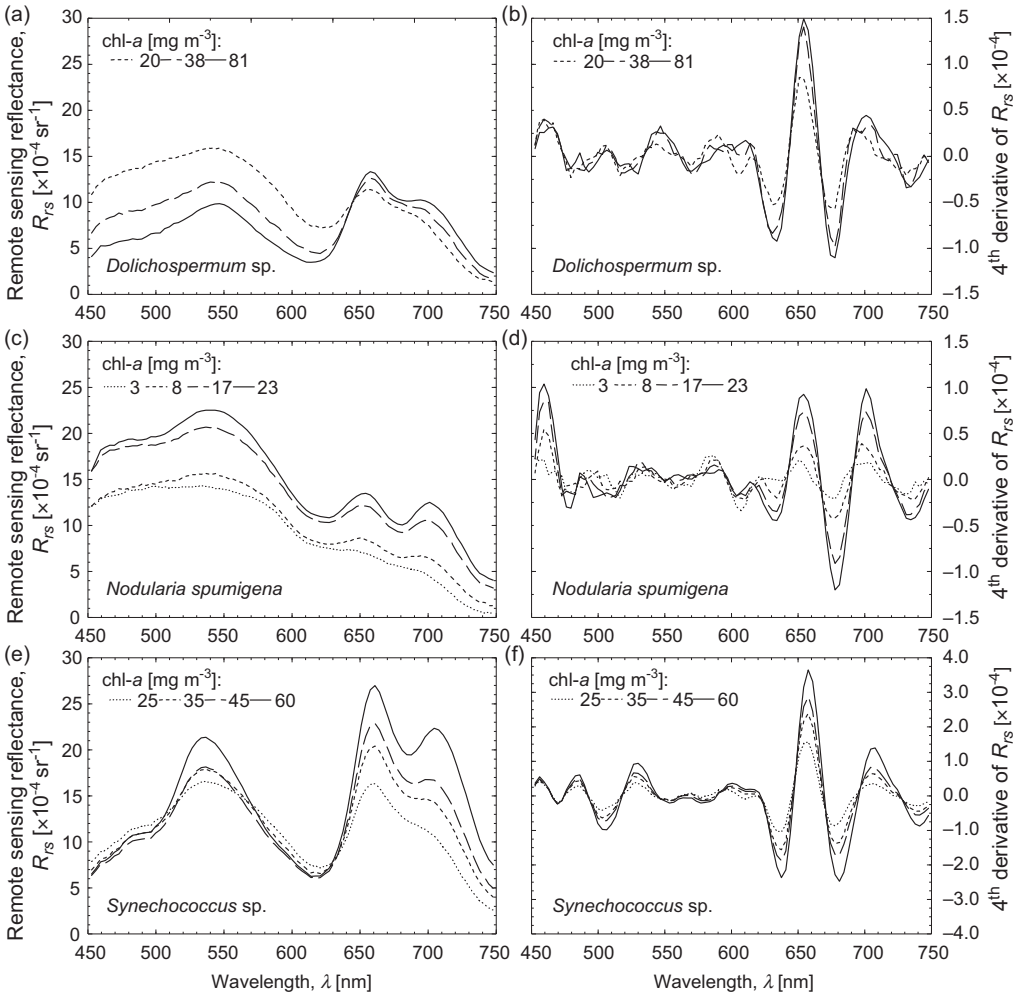

Figure 5 R_{rs} spectra and its 4th derivative for *Dolichospermum* sp. (a, b), *Nodularia spumigena* (c, d), and *Synechococcus* sp. (e, f), respectively.

cyanobacteria *Dolichospermum* sp. (Fig. 5), which suggests that absorption by pigments is a dominant process influencing shape of R_{rs} spectra. On the other hand, for the remaining species the scattering by particles played the dominant role in shaping the R_{rs} spectra causing the increase of the R_{rs} within this region with increasing chl-*a* concentration (Figs. 5 and 6). It needs to be noted that the increase in the phytoplankton concentration leads to increase of the impact of nonlinear effects on R_{rs}. Contribution of multiple scattering to radiance reflectance can be as high as 94% in turbid waters (Chami et al., 2006) what explains the changes in the spectral shape of R_{rs} observed with the increasing chl-*a* concentration (Figs. 5 and 6).

Besides the differences between the two phytoplankton groups, the R_{rs} spectra showed some differences between species belonging to the same group (Figs. 5 and 6). Among the diatoms the 700 nm peak in the R_{rs} is much more pronounced for *S. marinoi* compared to *C. meneghiniana* (Fig. 6). This was caused by differences in the scattering of light by these organisms resulting mainly from differences in their size and structure (Table 3). In the case of *S. marinoi* the shape of the R_{rs} spectrum changed distinctly with increasing chl-*a* concentration. It is probable that the number of cells was too small to have a sufficient impact on the R_{rs} spectrum. The differences observed among cyanobacteria strains (Fig. 5) resulted from the differences in their light scattering properties. For example, *N. spumigena* is characterised by almost wavelength independent scattering spectrum with low values of the chlorophyll-specific scattering coefficient (Metsamaa et al., 2006; Wojtasiewicz and Stoń-Egiert, 2016; Wojtasiewicz and Stramski, 2010). On the other hand, *Synechococcus* sp. cells are small therefore the scattering spectrum for this species is very steep and the scattering coefficient values are high (Wojtasiewicz and Stoń-Egiert, 2016). This can be the reason for a different shape of R_{rs} spectrum of *Synechococcus* sp. compared to the remaining ones.

Characteristic features of R_{rs} spectra for each species were the most evident for samples with the highest biomass of phytoplankton (chl-*a* as an indicator), what can clearly be seen by its 4th derivative changes (Figs. 5 and 6). These features were kept very well, with the SI $>$ 0.95, over concentrations of chl-*a* higher than 50% of maximum (Fig. 7). Higher dilution resulted in less distinct peaks, however SI for all analysed concentrations was higher than 0.6. The spectra which maintain their major features within wide range of chl-*a* concentration are suitable for developing model spectra for particular species. It is worth to note that characteristic shape of R_{rs} spectra for *N. spumigena* could be seen even if the

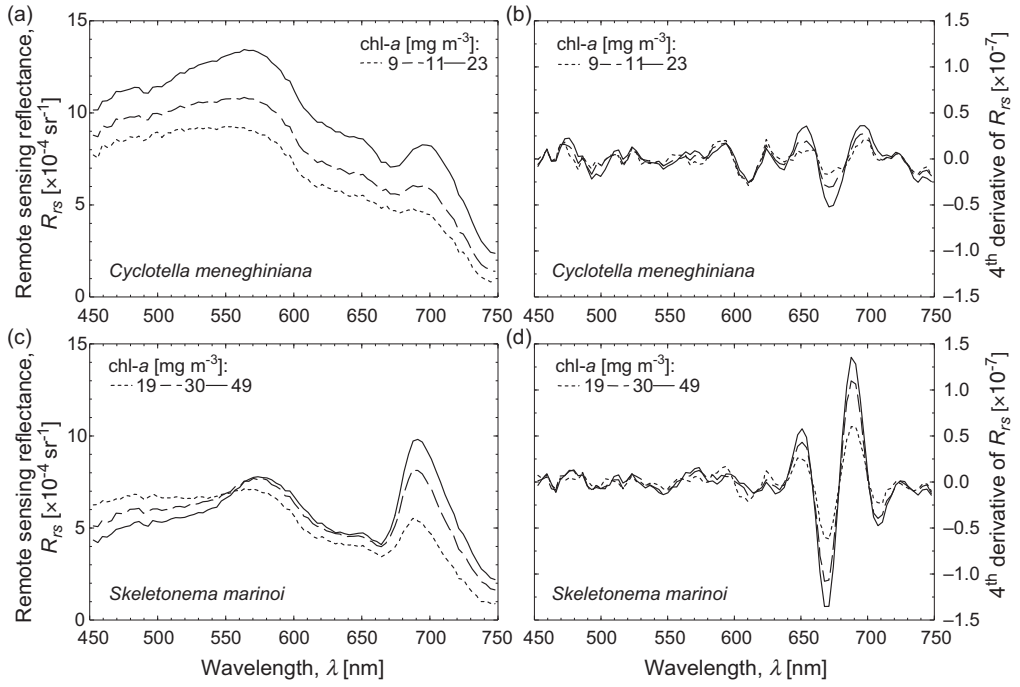

Figure 6 R_{rs} spectra and its 4th derivative for *Cyclotella meneghiniana* (a, b) and *Skeletonema marinoi* (c, d), respectively.

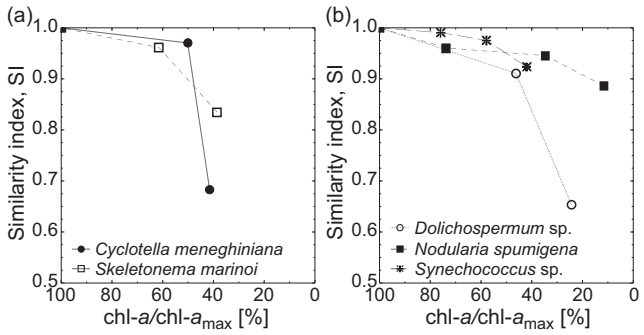

Figure 7 Similarity index between the R_{rs} spectra of phytoplankton species with increasing chl-*a* concentration.

concentration of chlorophyll *a* was relatively low, here it was only 13% of the reference concentration. It is due to the fact, that dilution of phytoplankton cells for this species results in changes of R_{rs} spectra magnitude rather than its shape (Fig. 5), despite slight shifts in the main peak positions. Similarly high dilution of cyanobacteria *Dolichospermum* or diatoms *S. marinoi* showed lower similarity to their references, with SI of about 0.65 (Fig. 7). This is a consequence of changes in relative height of peaks in blue-green and red portions of the R_{rs} spectra characteristic for these species (Figs. 5 and 6).

Characteristic features of R_{rs} spectra for different phytoplankton species described above are located at different bands over the whole analysed spectral range. Therefore to evaluate which phytoplankton species have the most unique optical signature, HCA between 450 nm and 750 nm was used. Fig. 8 illustrates the results from cluster analysis (HCA) applied to R_{rs} spectra presented in the left panels of Figs. 5 and 6. The spectra of picoplankton species, *Synechococcus* sp., for all concentration belonged to one cluster (Fig. 8), suggesting that those species have a distinct optical signature. The shape of R_{rs} spectra differed significantly from the other species. Two main peaks (close to 540 nm and 660 nm) were stable and similarly high for all studied concentrations. The second peak was shifted towards longer wavelengths compared to the other species, which had it around 650 nm. The second cluster (Fig. 8) included all *N. spumigena* spectra. However, it also contained one *Dolichospermum* sp. spectrum (lowest measured concentration) and one *C. meneghiniana* spectrum (highest measured concentration). Those spectra were characterised by three main peaks, where the second and the third peaks were significantly lower than the first one. Spectra of higher concentration of *Dolichospermum* sp. were characterised by higher second peak than the first one, and spectra of lower concentration of *C. meneghiniana* were flatter without distinct peaks. For those reasons they were not included in that group. The third cluster (Fig. 8) contained spectra of two diatom species, *C. meneghiniana* and *S. marinoi* and one cyanobacteria species, *Dolichospermum* sp. It is difficult to find any common features in the shape of their spectra except they are generally characterised by the lowest values of reflectance. However, if we considered clusters with similarity above 85% (the linkage distance decrease) the third cluster would be splitted into three separate groups, one for each species.

Summarising above, results of the HCA analysis based on R_{rs} showed that spectral signatures of *Synechococcus* sp., *N. spumigena* and *S. marinoi* were unique enough to separate each of them into different clusters regardless concentration. *Dolichospermum* sp. and *C. meneghiniana* showed similarity to *N. spumigena* or *S. marinoi*, depending on concentration (Fig. 8). Results of similar HCA analysis based on the 4th derivative of R_{rs} spectra gave worst results of

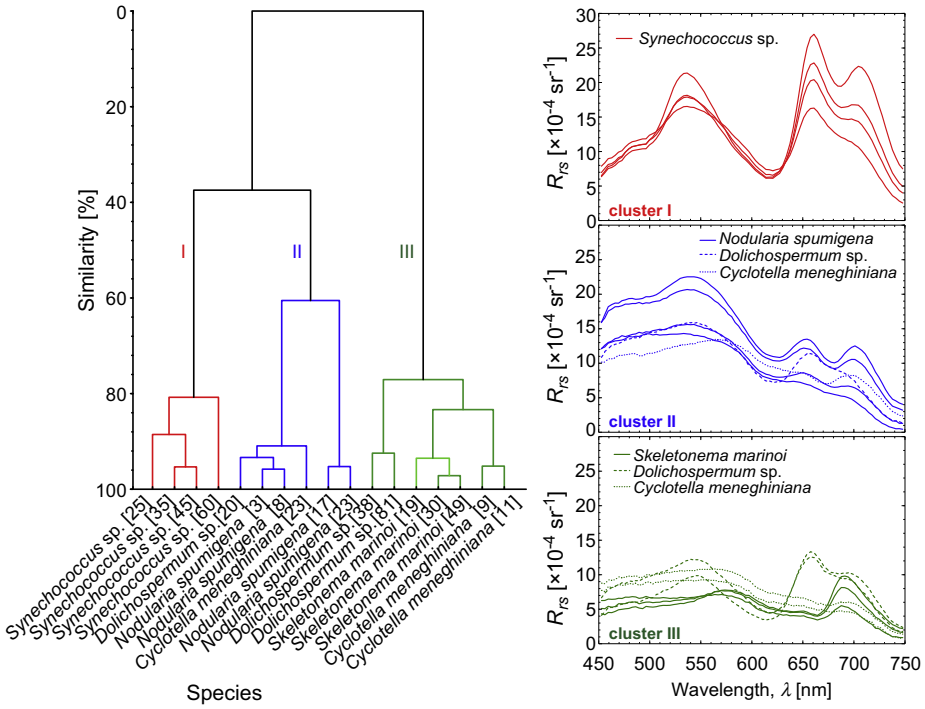

Figure 8 Cluster tree of all analysed phytoplankton species at different concentrations (chlorophyll *a* concentration in [mg m^{-3}] is given in parenthesis) generated by using $R_{rs}(\lambda)$ spectra in the range of 450—750 nm (left) and $R_{rs}(\lambda)$ spectra belonging to each cluster (right).

species separation. Although clusters in this case were characterised by higher inner similarity (three main clusters at level of 70% of similarity), spectra derived for the same species but with different chl-*a* concentration were placed in different clusters (*Synechococcus*, *Dolichospermum* sp. and *N. spumigena*) or if not, they belonged to one big cluster consisting spectra of different species (all *S. marinoi* and all *C. meneghiniana* together with some spectra of *N. spumigena* and *Dolichospermum* sp.). This fact showed that not only shape of R_{rs} spectrum (emphasised by the 4th derivative) but also its magnitude is an important feature. The clusters did not change if blue part of the spectrum (up to 525 nm) was excluded from the HCA analysis (525—750 nm analysed). In the blue part of a spectrum, R_{rs} is expected to be strongly modified in Baltic Sea waters, rich in dissolved organic matter.

4. Conclusions

The results from the unique experiments designed to study specific apparent optical properties of selected phytoplankton species of the Baltic Sea are shown in our paper. Presented reflectance spectra can be used in calibration and validation of radiative transfer models for water dominated by specific phytoplankton species. They can be successfully applied to modelling of the volume scattering function for phytoplankton assemblages (Woźniak, 2014). Moreover, the spectral shape characteristic for each species can be used as a reference spectrum for comparison with in situ measured reflectance spectra by means of similarity index (cosine similarity) or root-mean-square deviation. This can help to assess the water quality and distinguish the dominant phytoplankton type. There is a need for those data in development, calibration and validation of Earth Observation algorithms (Sathyendranath et al., 2016). We analysed the R_{rs} spectra of 5 phytoplankton species commonly occurring in the Baltic Sea. As expected, the pigment composition as well as size structure were responsible for differences in spectral shape of R_{rs} spectra. Beside the differences between the two phytoplankton groups, the R_{rs} spectra showed some differences between species belonging to one group. Their characteristic features, e.g. location of peaks and their relative heights, for each species were kept over wide range of phytoplankton concentrations with the similarity index (SI) higher than 0.6. The picoplankton species *Synechococcus* sp. showed the most distinct optical signature, which allowed to distinguish a separate cluster in HCA analysis. Presented study enlarges the database of existing specific optical properties of phytoplankton species in the Baltic Sea and shows the first step towards knowing the variability of R_{rs} within phytoplankton species. In further studies different phytoplankton growth phases and different conditions (light, temperature, nutrients, etc.) need to be accounted for.

Acknowledgements

The authors would like to thank colleagues from Division of Marine Biotechnology, and Division of Marine Ecosystems Functioning, both at the University of Gdańsk, for growing phytoplankton monocultures needed for experiments.

The work was supported as part of the Institute of Oceanography University of Gdańsk statutory research (DS/530-G210-D425) and the SatBaltyk project funded by the European Union through European Regional Development Fund (contract No. POIG.01.01.02-22-011/09 entitled 'The Satellite Monitoring of the Baltic Sea Environment'). M.S.-W. and B.W. were funded by CSIRO OCE Postdoctoral Fellowship Programme.

References

Aguirre-Gómez, R., Weeks, A.R., Boxall, S.R., 2001. The identification of phytoplankton pigments from absorption spectra. Int. J. Remote Sens. 22 (2–3), 315–338, http://dx.doi.org/10.1080/014311601449952.

Albertano, P., Somma, D.D., Capucci, E., 1997. Cyanobacterial picoplankton from the Central Baltic Sea: cell size classification by image-analyzed fluorescence microscopy. J. Plankton Res. 19 (10), 1405–1416, http://dx.doi.org/10.1093/plankt/19.10.1405.

Chami, M., McKee, D., Leymarie, E., Khomenko, G., 2006. Influence of the angular shape of the volume-scattering function and multiple scattering on remote sensing reflectance. Appl. Opt. 45 (36), 9210–9220, http://dx.doi.org/10.1364/AO.45.009210.

Craig, S.E., Lohrenz, S.E., Lee, Z., Mahoney, K.L., Kirkpatrick, G.J., Schofield, O.M., 2006. Use of hyperspectral remote sensing reflectance for detection and assessment of the harmful alga, *Karenia brevis*. Appl. Opt. 45 (21), 5414–5425, http://dx.doi.org/10.1364/AO.45.005414.

Darecki, M., Stramski, D., 2004. An evaluation of MODIS and SeaWiFS bio-optical algorithms in the Baltic Sea. Remote Sens. Environ. 89 (3), 326–350, http://dx.doi.org/10.1016/j.rse.2003.10.012.

Darecki, M., Ficek, D., Krężel, A., Ostrowska, M., Majchrowski, R., Woźniak, S.B., Bradtke, K., Dera, J., Woźniak, B., 2008. Algorithms for the remote sensing of the Baltic ecosystem (DESAMBEM). Part 2: Empirical validation. Oceanologia 50 (4), 509–538.

Evers-King, H., Bernard, S., Robertson-Lain, L., Probyn, T.A., 2014. Sensitivity in reflectance attributed to phytoplankton cell size: forward and inverse modelling approaches. Opt. Express 22 (10), 11536–11551, http://dx.doi.org/10.1364/OE.22.011536.

Feistel, R., Weinreben, S., Wolf, H., Seitz, S., Spitzer, P., Adel, B., Nausch, G., Schneider, B., Wright, D.G., 2010. Density and absolute salinity of the Baltic Sea 2006–2009. Ocean Sci. 6 (1), 3–24, http://dx.doi.org/10.5194/os-6-3-2010.

Gitelson, A., 1992. The peak near 700 nm on radiance spectra of algae and water: relationships of its magnitude and position with chlorophyll concentration. Int. J. Remote Sens. 13 (17), 3367–3373, http://dx.doi.org/10.1080/01431169208904125.

Gitelson, A.A., Schalles, J.F., Rundquist, D.C., Schiebe, F.R., Yacobi, Y.Z., 1999. Comparative reflectance properties of algal cultures with manipulated densities. J. Appl. Phycol. 11 (4), 345–354, http://dx.doi.org/10.1023/A:1008143902418.

Godhe, A., McQuoid, M.R., Karunasagar, I., Karunasagar, I., Rehnstam-Holm, A.-S., 2006. Comparison of three common molecular tools for distinguishing among geographically separated clones of the diatom *Skeletonema marinoi* Sarno et Zingone (Bacillariophyceae). J. Phycol. 42 (2), 280–291, http://dx.doi.org/10.1111/j.1529-8817.2006.00197.x.

Gordon, H.R., Brown, O.B., Jacobs, M.M., 1975. Computed relationships between the inherent and apparent optical properties of a flat, homogeneous ocean. Appl. Opt. 14 (2), 417–427, http://dx.doi.org/10.1364/AO.14.000417.

Hommersom, A., Kratzer, S., Laanen, M., Ansko, I., Ligi, M., Bresciani, M., Giardino, C., Beltrán-Abaunza, J.M., Moore, G., Wernand, M., Peters, S., 2012. Intercomparison in the field between the new WISP-3 and other radiometers (TriOS Ramses, ASD FieldSpec, and TACCS). J. Appl. Remote Sens. 6 (1), 063615, http://dx.doi.org/10.1117/1.JRS.6.063615 21pp.

Hunter, P.D., Tyler, A.N., Présing, M., Kovács, A.W., Preston, T., 2008. Spectral discrimination of phytoplankton colour groups: the effect of suspended particulate matter and sensor spectral resolution. Remote Sens. Environ. 112 (4), 1527–1544, http://dx.doi.org/10.1016/j.rse.2007.08.003.

IOCCG, 2014. Phytoplankton functional types from space. In: Sathyendranath, S. (Ed.), Reports of the International Ocean-Colour Coordinating Group, No. 15. IOCCG, Dartmouth, Canada, Phytoplankton functional types from Space, 156 pp.

Jain, A.K., Murty, M.N., Flynn, P.J., 1999. Data clustering: a review. ACM Comput. Surv. 31 (3), 264–323, http://dx.doi.org/10.1145/331499.331504.

Jeffrey, S.W., Humphrey, G.F., 1975. New spectrophotometric equations for determining chlorophylls *a*, *b*, *c1*, and *c2* in higher plants, algae and natural phytoplankton. Biochem. Physiol. Pflanz. 167, 191–194, http://dx.doi.org/10.1016/S0015-3796(17)30778-3.

Kahru, M., 1997. Using satellites to monitor large-scale environmental change: a case study of cyanobacteria blooms in the Baltic Sea. In: Kahru, M., Brown, C.W. (Eds.), Monitoring Algal Blooms: New Techniques for Detecting Large-scale Environmental Change. Springer, Berlin/New York, 43–61.

Kanoshina, I., Lips, U., Leppänen, J.-M., 2003. The influence of weather conditions (temperature and wind) on cyanobacterial bloom development in the Gulf of Finland (Baltic Sea). Harmful Algae 2 (1), 29–41, http://dx.doi.org/10.1016/S1568-9883(02)00085-9.

Karlsson, K.M., Kankaanpää, H., Huttunen, M., Meriluoto, J., 2005. First observation of microcystin-LR in pelagic cyanobacterial blooms in the northern Baltic Sea. Harmful Algae 4 (1), 163–166, http://dx.doi.org/10.1016/j.hal.2004.02.002.

Kim, Y., Yoo, S., Son, Y.B., 2016. Optical discrimination of harmful *Cochlodinium polykrikoides* blooms in Korean coastal waters. Opt. Express 24 (22), A1471, http://dx.doi.org/10.1364/OE.24.0A1471, 18 pp.

Klais, R., Tamminen, T., Kremp, A., Spilling, K., An, B.W., Hajdu, S., Olli, K., 2013. Spring phytoplankton communities shaped by interannual weather variability and dispersal limitation: mechanisms of climate change effects on key coastal primary producers. Limnol. Oceanogr. 58 (2), 753–762, http://dx.doi.org/10.4319/lo.2013.58.2.0753.

Kratzer, S., Brockmann, C., Moore, G., 2008. Using MERIS full resolution data to monitor coastal waters – a case study from Himmerfjärden, a fjord-like bay in the north-western Baltic Sea. Remote Sens. Environ. 112 (5), 2284–2300, http://dx.doi.org/10.1016/j.rse.2007.10.006.

Kutser, T., Metsamaa, L., Strömbeck, N., Vahtmäe, E., 2006. Monitoring cyanobacterial blooms by satellite remote sensing. Estuar. Coast. Shelf Sci. 67 (1–2), 303–312, http://dx.doi.org/10.1016/j.ecss.2005.11.024.

Kutser, T., Paavel, B., Verpoorter, C., Ligi, M., Soomets, T., Toming, K., Casal, G., 2016. Remote sensing of black lakes and using 810 nm reflectance peak for retrieving water quality parameters of optically complex waters. Remote Sens. 8 (6), 497, http://dx.doi.org/10.3390/rs8060497, 15 pp.

Lewandowska, J., Kosakowska, A., 2004. Effect of iron limitation on cells of the diatom *Cyclotella meneghiniana* Kutzing. Oceanologia 46 (2), 269–287.

Lubac, B., Loisel, H., Guiselin, N., Astoreca, R., Artigas, L.F., Mériaux, X., 2008. Hyperspectral and multispectral ocean color inversions to detect *Phaeocystis globosa* blooms in coastal waters. J. Geophys. Res. 113 (C6), http://dx.doi.org/10.1029/2007JC004451, 17 pp.

Mazur, H., Pliński, M., 2003. *Nodularia spumigena* blooms and the occurrence of hepatotoxin the Gulf of Gdańsk. Oceanologia 45 (1), 305–316.

Mazur-Marzec, H., Krężel, A., Kobos, J., Pliński, M., 2006. Toxic *Nodularia spumigena* blooms in the coastal waters of the Gulf of Gdańsk: a ten-year survey. Oceanologia 48 (2), 255–273.

Metsamaa, L., Kutser, T., Strömbeck, N., 2006. Recognising cyanobacterial blooms based on their optical signature: a modelling study. Boreal Environ. Res. 11, 493–506, 14 pp.

Millie, D.F., Schofield, O.M., Kirkpatrick, G.J., Johnsen, G., Tester, P.A., Vinyard, B.T., 1997. Detection of harmful algal blooms using photopigments and absorption signatures: a case study of the FLorida red tide dinoglagellate, *Gymnodinium breve*. Limnol. Oceanogr. 42 (5), 1240–1251, http://dx.doi.org/10.4319/lo.1997.42.5_part_2.1240.

Millie, D.F., Schofield, O.M.E., Kirkpatrick, G.J., Johnsen, G., Evens, T.J., 2002. Using absorbance and fluorescence spectra to

discriminate microalgae. Eur. J. Phycol. 37 (3), 313–322, http://dx.doi.org/10.1017/S0967026202003700.

Nowacki, J., Jarosz, E., 1998. The hydrological and hydrochemical division of the surface waters in the Gulf of Gdańsk. Oceanologia 40 (3), 261–272.

Olenina, I., Hajdu, S., Edler, L., Andersson, A., Wasmund, N., Busch, S., Göbel, J., Gromisz, S., Huseby, S., Huttunen, M., Jaanus, A., Kokkonen, P., Ledaine, I., Niemkiewicz, E., 2006. Biovolumes and size-classes of phytoplankton in the Baltic Sea (Proceedings No. 106). In: HELCOM Baltic Sea Environment Proceedings. HELCOM, Helsinki, 144 pp.

Oyama, Y., Matsushita, B., Fukushima, T., Chen, J., Nagai, T., Imai, A., 2010. Testing the spectral decomposition algorithm (SDA) for different phytoplankton species by a simulation based on tank experiments. Int. J. Remote Sens. 31 (6), 1605–1623, http://dx.doi.org/10.1080/01431160903475365.

Pankow, H., Kell, V., Wasmund, N., Zander, B., 1990. Ostsee-Algenflora. G. Fischer Verl, Jena, 85 pp.

Parsons, T.R., Maita, Y., Lalli, C.M., 1984. A Manual of Chemical and Biological Methods for Seawater Analysis. Pergamon Press, Oxford, 173 pp.

Pliński, M., Mazur-Marzec, H., Jóźwiak, T., Kobos, J., 2007. The potential causes of cyanobacterial blooms in Baltic Sea estuaries. Oceanol. Stud. 36 (1), 125–137, http://dx.doi.org/10.2478/v10009-007-0001-x.

Rabinowitch, E., Govindjee, 1969. Photosynthesis. John Wiley and Sons, Inc., New York/London/Sydney/Toronto, 273 pp.

Roy, S., Llewellyn, C.A., Skarstad-Egeland, E., Johnsen, G., 1989. Phytoplankton Pigments Characterization, Chemotaxonomy and Applications in Oceanography (Cambridge Environmental Chemistry Series). Cambridge Univ. Press, Cambridge, New York, 845 pp.

Sathyendranath, S., Bracher, A., Brockmann, C., Platt, T., Ramon, D., Regner, P., 2016. Colour and Light in the Ocean (CLEO) 2016: A Scientific Roadmap from the CLEO Workshop Organised by ESA and PML. Frascati, Italy, 77 pp.

Seppälä, J., Ylöstalo, P., Kaitala, S., Hällfors, S., Raateoja, M., Maunula, P., 2007. Ship-of-opportunity based phycocyanin fluorescence monitoring of the filamentous cyanobacteria bloom dynamics in the Baltic Sea. Estuar. Coast. Shelf Sci. 73 (3–4), 489–500, http://dx.doi.org/10.1016/j.ecss.2007.02.015.

Shang, S., Wu, J., Huang, B., Lin, G., Lee, Z., Liu, J., Shang, S., 2014. A new approach to discriminate dinoflagellate from diatom blooms from space in the East China Sea. J. Geophys. Res. Oceans 119 (7), 4653–4668, http://dx.doi.org/10.1002/2014JC009876.

Simis, S.G.H., Peters, S.W.M., Gons, H.J., 2005. Remote sensing of the cyanobacterial pigment phycocyanin in turbid inland water. Limnol. Oceanogr. 50 (1), 237–245, http://dx.doi.org/10.4319/lo.2005.50.1.0237.

Smith, R.C., Baker, K.S., 1981. Optical properties of the clearest natural waters (200–800 nm). Appl. Opt. 20 (2), 177–184, http://dx.doi.org/10.4319/lo.2007.52.1.0217.

Sobiechowska-Sasim, M., Stoń-Egiert, J., Kosakowska, A., 2014. Quantitative analysis of extracted phycobilin pigments in cyanobacteria – an assessment of spectrophotometric and spectrofulorometric methods. J. Appl. Phycol. 26 (5), 2065–2074, http://dx.doi.org/10.1007/s10811-014-0244-3.

Soja-Woźniak, M., Craig, S., Kratzer, S., Wojtasiewicz, B., Darecki, M., Jones, C., 2017. A novel statistical approach for ocean colour estimation of inherent optical properties and cyanobacteria abundance in optically complex waters. Remote Sens. 9 (4), 343, http://dx.doi.org/10.3390/rs9040343, 22 pp.

Suikkanen, S., Laamanen, M., Huttunen, M., 2007. Long-term changes in summer phytoplankton communities of the open northern Baltic Sea. Estuar. Coast. Shelf Sci. 71 (3–4), 580–592, http://dx.doi.org/10.1016/j.ecss.2006.09.004.

Torrecilla, E., Stramski, D., Reynolds, R.A., Millán-Núñez, E., Cannizzaro, J., 2011. Cluster analysis of hyperspectral optical data for discriminating phytoplankton pigment assemblages in the open ocean. Remote Sens. Environ. 115 (10), 2578–2593, http://dx.doi.org/10.1016/j.rse.2011.05.014.

Townend, J., 2002. Practical Statistics for Environmental and Biological Scientists. Wiley, Chichester/New York, 276 pp.

Vaillancourt, R.D., Brown, C.W., Guillard, R.R.L., Balch, W.M., 2004. Light backscattering properties of marine phytoplankton: relationships to cell size, chemical composition and taxonomy. J. Plankton Res. 26 (2), 191–212, http://dx.doi.org/10.1093/plankt/fbh012.

Volten, H., de Haan, J.F., Hovenier, J.W., Schreurs, R., Vassen, W., Dekker, A.G., Hoogenboom, H.J., Charlton, F., Wouts, R., 1998. Laboratory measurements of angular distributions of light scattered by phytoplankton and silt. Limnol. Oceanogr. 43 (6), 1180–11970, http://dx.doi.org/10.4319/lo.1998.43.6.1180.

Walsby, A.E., Hayes, P.K., Boje, R., 1995. The gas vesicles, buoyancy and vertical distribution of cyanobacteria in the Baltic Sea. Eur. J. Phycol. 30 (2), 87–94, http://dx.doi.org/10.1080/09670269500650851.

Warner, R.A., Fan, C., 2013. Optical spectra of phytoplankton cultures for remote sensing applications: focus on harmful algal blooms. Int. J. Environ. Sci. Dev. 4 (2), 94–98, http://dx.doi.org/10.7763/IJESD.2013.V4.312.

Whitmire, A.L., Pegau, W.S., Karp-Boss, L., Boss, E., Cowles, T.J., 2010. Spectral backscattering properties of marine phytoplankton cultures. Opt. Express 18 (14), 15073–15093, http://dx.doi.org/10.1364/OE.18.015073.

Wojtasiewicz, B., Stoń-Egiert, J., 2016. Bio-optical characterization of selected cyanobacteria strains present in marine and freshwater ecosystems. J. Appl. Phycol. 28 (4), 2299–2314, http://dx.doi.org/10.1007/s10811-015-0774-3.

Wojtasiewicz, B., Stramski, D., 2010. Chlorophyll-specific absorption and scattering coefficients of selected cyanobacteria. In: Proceedings of Ocean Optics XX.

Woźniak, M., 2014. Identification of the dominant phytoplankton groups in the algal blooms in the waters of the Baltic Sea using remote sensing methods. (PhD). Univ. Gdańsk, Gdynia, 153 pp. (in Polish).

Woźniak, B., Krężel, A., Darecki, M., Woźniak, S.B., Majchrowski, R., Ostrowska, M., Kozłowski, Ł., Ficek, D., Olszewski, J., Dera, J., 2008. Algorithms for the remote sensing of the Baltic ecosystem (DESAMBEM). Part 1: Mathematical apparatus. Oceanologia 50 (4), 451–508.

Woźniak, M., Bradtke, K.M., Darecki, M., Krężel, A., 2016. Empirical model for phycocyanin concentration estimation as an indicator of cyanobacterial bloom in the optically complex coastal waters of the Baltic Sea. Remote Sens. 8 (3), http://dx.doi.org/10.3390/rs8030212, 23 pp.

Wright, S.W., Jeffrey, S.W., 1987. Fucoxanthin pigment markers of marine phytoplankton analysed by HPLC and HPTLC. Mar. Ecol.-Prog. Ser. 38, 259–266.

Xi, H., Hieronymi, M., Röttgers, R., Krasemann, H., Qiu, Z., 2015. Hyperspectral differentiation of phytoplankton taxonomic groups: a comparison between using remote sensing reflectance and absorption spectra. Remote Sens. 7 (11), 14781–14805, http://dx.doi.org/10.3390/rs71114781.

Zibordi, G., Darecki, M., 2006. Immersion factor for the RAMSES series of hyperspectral underwater radiometers. J. Opt. Pure Appl. Opt. 8, 252–258.